Arabian Journal of Chemistry (2022) **15**, 103658

King Saud University

Arabian Journal of Chemistry

www.ksu.edu.sa
www.sciencedirect.com

ORIGINAL ARTICLE

The surface modification of spherical ZnO with Ag nanoparticles: A novel agent, biogenic synthesis, catalytic and antibacterial activities

Reza Fouladi-Fard [a], Rahim Aali [a], Sarvin Mohammadi-Aghdam [b], Sobhan Mortazavi-derazkola [c,*]

[a] *Research Center for Environmental Pollutants, Department of Environmental Health Engineering, Faculty of Health, Qom University of Medical Sciences, Iran*
[b] *Department of Chemistry, Payame Noor University, P.O. BOX 19395-3697, Tehran, Iran*
[c] *Medical Toxicology and Drug Abuse Research Center (MTDRC), Birjand University of Medical Sciences, Birjand, Iran*

Received 2 November 2021; accepted 16 December 2021
Available online 21 December 2021

KEYWORDS

Green synthesis;
Photocatalytic degradation;
Antibacterial;
ZnO nanoparticles

Abstract Nowadays, the industrial wastewater pollutants including toxic dyes and pathogenic microbes have caused serious environmental contaminations and human health problems. In the present study, eco-friendly and facile green synthesis of Ag modified ZnO nanoparticles (ZnO-Ag NPs) using *Crataegus monogyna* (*C. monogyna*) extract (ZnO-Ag@CME NPs) is reported. The morphology and structure of the as-biosynthesized product were characterized by field emission scanning electron microscopy (FESEM), X-Ray diffraction (XRD), differential reflectance spectroscopy (DRS), dynamic light scattering (DLS), transmission electron microscopy (TEM), Fourier-transform infrared spectroscopy (FT-IR), and energy-dispersive X-ray spectroscopy (EDS) techniques. TEM and FESEM images confirmed the oval and spherical-like structure of the products with a size of 55–70 nm. The EDS analysis confirmed the presence of Zn, Ag, and O elements in the biosynthesized product. The photocatalytic results showed ZnO-Ag@CME NPs were degraded (89.8% and 75.3%) and (94.2% and 84.7%) of methyl orange (MO) and basic violet 10 (BV10), under UV and sunlight irradiations, respectively. The Ag modified ZnO nanoparticles exhibited enhanced catalytic activity towards organic pollutants, and showed better performance than the pure ZnO nanoparticles under UV and sunlight irradiations. This performance was probably due to the presence of silver nanoparticles as a plasmonic material. Antibacterial activity was performed against different bacteria. ZnO-Ag@CME NPs showed high antibacterial activity against *K. pneumoniae*, *S. typhimurium*, *P. vulgaris*, *S. mitis*, and *S. faecalis* with MIC values

* Corresponding author.
E-mail address: Sobhan.mortazavi@bums.ac.ir (S. Mortazavi-derazkola).
Peer review under responsibility of King Saud University.

Production and hosting by Elsevier

https://doi.org/10.1016/j.arabjc.2021.103658

of 50, 12.5, 12.5, 12.5, and 12.45 μg/mL, respectively. All in all, the present investigation suggests a promising method to achieve high-efficiency antibacterial and catalytic performance.

1. Introduction

Nanotechnology is developing fields that seek to manipulate and design material ranges under 100 nm at least in one dimension. This field reveals unique properties of matter at the nanoscale and emerges in all fields of science in order to develop new capabilities and properties. The improvement of nanotechnology has led the develop approaches in the synthesis of nanoparticles that are useful in numerous fields such as medicine (Mohammadi-Aghdam et al., 2019; Ghoreishi et al., 2017; Mortazavi-Derazkola et al., 2016; Ardestani et al., 2020), engineering (Nga et al., 2018; Zulkifli et al., 2017; Kiani et al., 2019), environmental (Heinemann et al., 2021; Ebrahimzadeh et al., 2019; Naghizadeh et al., 2021; Eslami et al., 2019; Salehi et al., 2020), pharmaceutical (Alomar et al., 2020), and biotechnology (Mehta, 2017; Ghanbari et al., 2016; Joulaei et al., 2019). Modern medicine has been impressed by the nanoscale materials that are involved in diagnosis and therapy. Unique features of nanomaterials such as high surface to volume ratio, multimodality, quantum properties and their ability to adsorb and carry other compounds, distinguished them from bulk materials.

Zinc oxide (ZnO) is an n-type semiconductor inorganic compound with interesting electronic, chemical, and optical properties. Due to the unique properties of these nanoparticles, such as non-toxic inorganic compound, zinc oxide nanoparticles is a promising candidate for use in cosmetics and pharmaceutical products (Shaikshavali et al., 2020; Sridar et al., 2018). In addition, more studies showed that ZnO nanoparticles have a lot of potential in biomedical fields due to the anti- bacterial, anti-fungal, anti-cancer, drug delivery, and gene delivery (Suba et al., 2021; Perveen et al., 2020; Kumar et al., 2013). Tiwari and co-workers investigated the anti-bacterial effect of ZnO nanoparticles against carbapenem-resistant *Acinetobacter baumannii*. They claim that the mechanism might be due to the creation of reactive oxygen species (ROS). ROS causes lipid peroxidation, followed by DNA and protein leakage, and ultimately reduced cell viability (Tiwari et al., 2018). Akbari *et al.* published the new pH-sensitive nanocomposite based on carboxymethyl cellulose (CMC) and ZnO nanoparticles as a drug delivery system. They state that this nano-carrier has an effective potential on sustained and control release of drug (Zare-Akbari et al., 2016).

Besides Zinc, silver (Ag) has been noticed due to their high activity against bacteria, viruses, fungal, microorganisms, and cancer (Shirzadi-Ahodashti et al., 2021; Shirzadi-Ahodashti et al., 2020; Yilmaz et al., 2020; Ebrahimzadeh et al., 2021). Therefore, studies on silver nanoparticles, and beneficial Ag nanoparticles properties on medicine and human health have been considered. Different properties of Ag nanoparticles have been discovered in the medical field, including medical devices, biosensors, and drug delivery systems. Also, these nanoparticles are high expectations for suppressing multidrug-resistant on wide range of anti-bacterial and viral spectrum. Yin & co-worker reported that silver nanoparticles have broad spectrum ability of anti- bacterial, fungal, and virial properties. They claimed that this ability may attribute to bacterial cell walls penetration, changing the cell membrane, production of ROS, and also interrupt replication of deoxyribonucleic acid by releasing silver ions (Yin et al., 2020).

It can be concluded that the merge of two inorganic compounds is interesting due to the broad applications of Ag and ZnO nanoparticles. Wang *et al.* reported that the ZnO-Ag composite photocatalysts were synthesized via the deposition of Ag on the surface of the grassy ZnO. Results showed that ZnO/Ag composites had tremendous photocatalytic efficiency in decolorization of rhodamine b contaminant under UV irradiation (Wang et al., 2021). Pandiyan & co-workers synthesized the Ag-Au/ZnO nanostructure, and anti-bacterial and cancer effects were investigated. They stated that bi-metal nanoparticles improved the biomedical properties (Pandiyan et al., 2019).

While nanotechnology is developing in all aspects of science, safety approaches that harmful effect on the environment, have been considered. Various chemical and physical methods are used to synthesize and produce nanoparticles. However, the high costs, environmental pollution, and production of hazardous products to living organisms have changed the point of view of synthesizing process. Therefore, researchers have been fascinated by new methods including plant extract, bacteria, fungi, and yeast to synthesize the nanoparticles so-called "green synthesize" (Alabdallah and Hasan, 2021; Moraes et al., 2021; Gonca et al., 2021; Kaplan et al., 2021). This is the cost-effective method that gives us the chance to produce nanoparticles with less negative effect on environment and human health. Khatami *et al.* published the application of green synthesized Ag, ZnO, and Ag/ZnO nanoparticles as a clinical antimicrobial agent in wound-healing bandages. The results showed that these nanoparticles have a promising antimicrobial effects, and they can be used for treating diabetic or burn wounds (Khatami et al., 2018). Manjari & co-workers reported the facile green synthesis of Ag–Cu decorated ZnO nanocomposite for detection of nitrite ions, and removal of other toxic organic compounds. The catalytic result of this nanocomposite exhibited good performance for the elimination of toxic organic compounds (Manjari et al., 2020).

The anionic and cationic contaminants (organic pollutants) are some of the most important environmental contaminants that are applied in various industries such as paper printing, rubber, textile, etc. (Şahin et al., 2013; , 2014). The photocatalytic degradation technique is one of the beneficial methods that have been done for dye removal from wastewater. Photocatalytic process indicates the potential impact on the widespread spectrum of pollutant mineralization. Therefore, green nanomaterials are recently achieved a great attention in order to degradation of environmental pollutants such as SnO_2 (Najjar et al., 2021), ZnO (Vasantharaj et al., 2021), palladium (Olajire and Mohammed, 2019), Ag@Fe (Al-Asfar et al., 2018), TiO_2 (Goutam et al., 2018), etc. In recent years, various plants were applied for the fabrication of nanoparticles which showed promising biological and catalytic activities (Table. 1).

In the present research, we report a facile and green synthesis of ZnO-Ag nanoparticles using C. *monogyna* extract and obtained products were characterized using various techniques. The photocatalytic performance of the biosynthesized nanoparticles (pure ZnO and ZnO-Ag) were calculated by using methyl orange (MO) as an anionic pollutant and basic violet 10 (BV10) as a cationic pollutant under UV and sunlight irradiations. Furthermore, the antibacterial activity of synthesized nanoparticles was investigated against Gram-positive and Gram-negative microorganisms. In doing so, we provided a green and cost-effective process for the synthesis of ZnO-Ag nanoparticles. Enhanced efficiency of spherical-like ZnO-Ag@CME NPs as nanocatalyst for degradation contaminants under UV and sunlight irradiations and high antibacterial activity against various microorganisms are some of the novelty of this research.

2. Experimental

2.1. Chemicals

$Zn(NO_3)_2{\cdot}6H_2O$ (Zinc nitrate hexahydrate), silver nitrate ($AgNO_3$), sodium hydroxide (NaOH), methanol, and ethanol

Table 1 The nanomaterials prepared from various plants by different researchers.

Sample no.	Plant	Part	Product	Application	References
1	*Opuntia humifusa*	Fruit	ZnO	Antibacterial activity	(Chennimalai et al., 2021)
2	*Syzygium cumini*	Leaf	ZnO	Antioxidants, cytotoxic activities	(Arumugam et al., 2021)
3	*Hibiscus rosa-sinensis*	Leaf	Fe-ZnO	Catalytic and antibacterial activities	(Lam et al., 2021)
4	*Salvia officinalis*	Leaf	Ag-Fe	Catalytic activity	(Malik et al., 2021)
5	*Justicia adhatoda*	Leaf	Ag-Au/Y_2O_3	Antibacterial and anticancer activities	(Pandiyan et al., 2021)
6	*Ramaria botrytis*	Fruit	Ag@Au	Catalytic, antioxidant and antibacterial activities	(Bhanja et al., 2020)
7	*Acacia nilotica*	Leaf	Ag/TiO_2	Antimicrobial and anticancer activity	(Rao et al., 2019)
8	*Morus alba L.*	Leaf	$CuFe_2O_4$	Catalytic activity	(Cahyana et al., 2021)
9	*Trigonella foenum-graecum*	Leaf	Ag-ZnO	Antibacterial, antifungal, antioxidant and catalytic activities	(Noohpisheh et al., 2020)
10	*Vitis vinifera*	Leaf	ZnO-Ag	Catalytic and antibacterial activities	(Saravanadevi et al., 2020)

were purchased from Sigma-Aldrich Company and applied without further purification. Antibacterial properties were investigated against different bacteria such as *Salmonella typhimurium* (*S. typhimurium*; ATCC 14028), *Klebsiella pneumoniae* (*K. pneumoniae*; ATCC 9997), *Proteus vulgaris* (*P. vulgaris*; ATCC 6380), *Pseudomonas aeruginosa* (*P. aeruginosa*; ATCC 27853), *Streptococcus mitis* (*S. mitis*; ATCC 6249), *Streptococcus salivarius* (*S. salivarius*; ATCC 1448), *Streptococcus faecalis* (*S. faecalis*; ATCC 15753) and *Streptococcus aureus* (*S. aureus*; ATCC 16538).

2.2. Preparation of *C. monogyna* extract

The procedure followed for the preparation of extract was according to the earlier literature (Ebrahimzadeh et al., 2020). The fruits of *Crataegus monogyna* were collected from the forests of Mazandaran province of Iran and thoroughly washed several times with distilled water. The methanolic extract was prepared as follows: 150 g of fruit was extracted through the maceration process using 400 mL of methanol as extraction solvent at room temperature. After concentrating the extract with rotary vacuum, the extract was isolated from solids through filtration using Whatman filter paper and stored at 4 ℃. The final extract was used as reducing, stabilizing, and capping agents.

2.3. Synthesis of ZnO nanoparticles (ZnO NPs)

Zinc oxide nanoparticles were synthesized by a simple and fast co-precipitation method. ZnO nanoparticles were obtained by modification of the method described by Wang *et al.* (Wang et al., 2021). In a typical procedure, 0.08 mol of zinc nitrate (1.19 g) was dissolved in 30 mL deionized water under vigorous stirring at room temperature, and then ammonium hydroxide (25% w/w) was added until the solution becomes pH12 and milky color. The final milky product was washed with DI water and ethanol three times, and dried at 70 ℃ for 24 h. The final ZnO nanoparticles were obtained by calcining at 500 ℃ for 3 h. The mechanism of zinc oxide preparation through the reaction of ammonium hydroxide with dissolved Zn^{2+} ions can be summarized as follow:

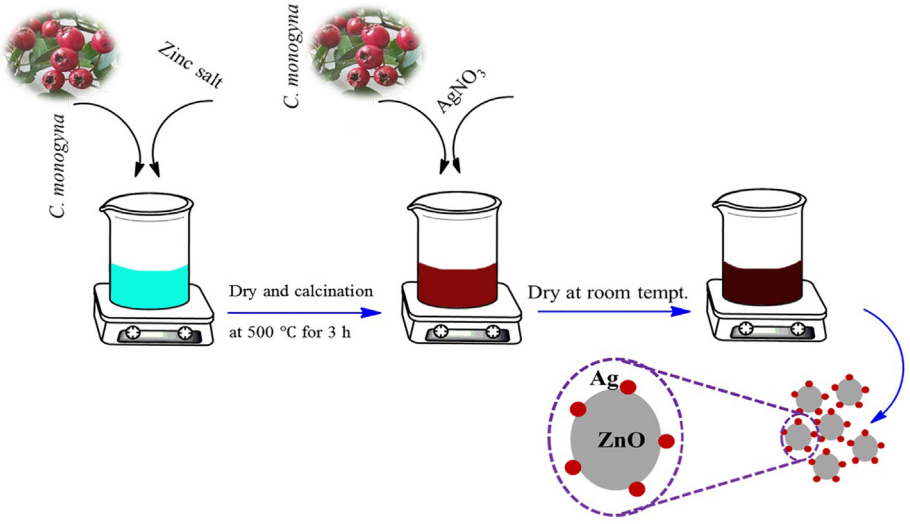

Scheme 1 Schematic illustration for green synthesis of ZnO-Ag biosynthesized using *C. monogyna*.

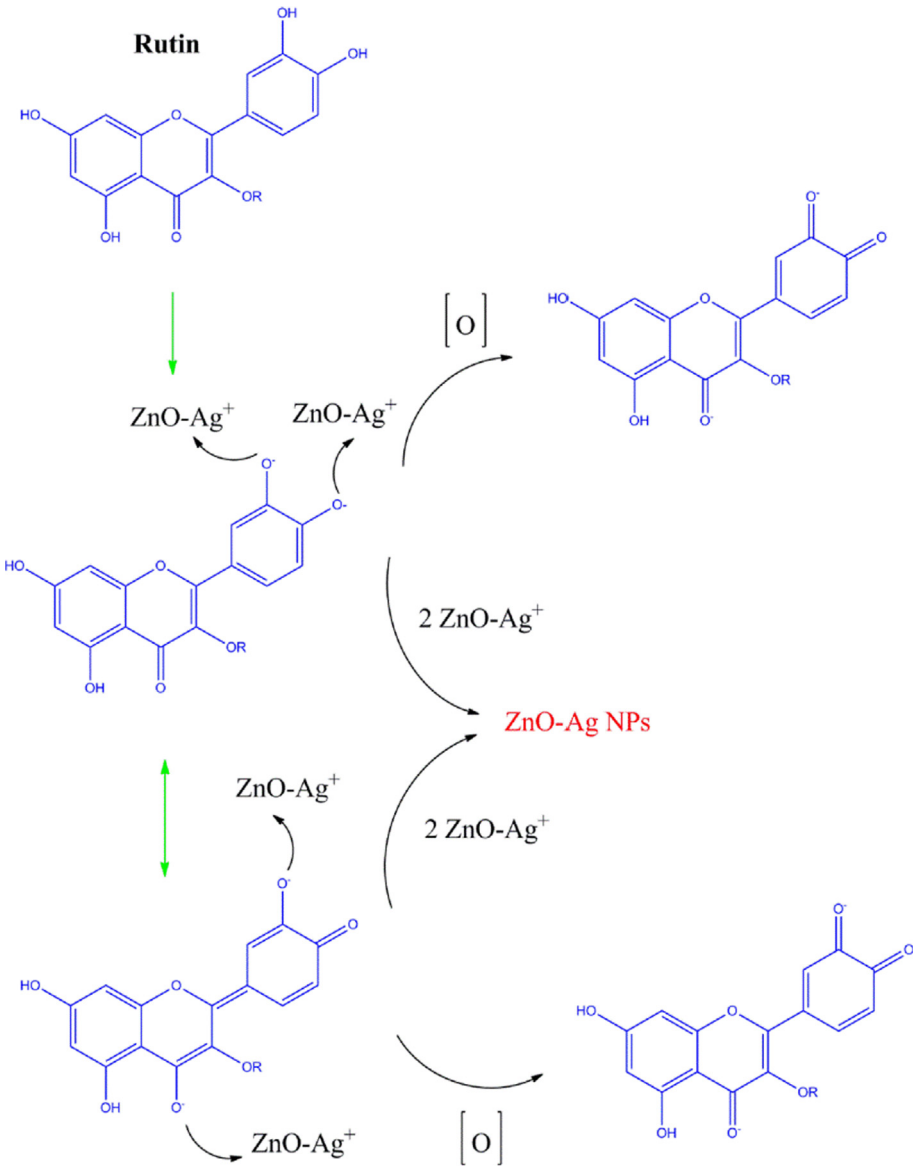

Fig. 1 The possible mechanism of the bio-synthesized of ZnO-Ag using *C. monogyna* extract.

$$NH_3 + H_2O \leftrightarrow NH_4^+ + OH^- \quad (1)$$

$$Zn^{2+} + 4NH_3 \leftrightarrow [Zn(NH_3)_4]^{2+} \rightarrow ZnO + 4NH_3 + 2H_2O \quad (2)$$

$$Zn[(NH_3)_4]^{2+} + 4OH^- \rightarrow [(Zn(OH)_4]^{2-} + 4NH_3 \quad (3)$$

$$Zn^{2+} + 4OH^- \leftrightarrow [Zn(OH)_4]^{2-} \leftrightarrow ZnO + H_2O + 2OH^- \quad (4)$$

2.4. Biosynthesis of ZnO-Ag nanoparticles (ZnO-Ag@CME NPs)

The ZnO-Ag nanoparticles were prepared according to the previous literature with a slight change (Manjari et al., 2020). Biosynthesis of ZnO-Ag was done by the following procedure: 0.1 g of the synthesized spherical ZnO nanoparticles was dispersed in 20 mL of deionized water and 10 mL of ethanol solution by ultrasound sonication for 30 min. After that, 15 mL of 0.002 M of silver nitrate ($AgNO_3$) was added to the above-dispersed ZnO solution under vigorous stirring for 20 min. Next, 7 mL of extract (pH 12 with NaOH) as stabilizing, reducing, and capping agents was added to above solution. Finally, the precipitate was collected and washed three times with ethanol and deionized water to drain out the excess ions (like nitrate) from the solution. Finally, the obtained product was dried (at room temperature) well for further characterization and applications (Scheme 1). The suggested mechanism for the preparation of ZnO-Ag nanoparticles in presence of C. *monogyna* extract is presence of Fig. 1.

2.5. Anti-bacterial activity

In this research various microorganisms were used such as *P. aeruginosa, K. pneumoniae, S. typhimurium, P. vulgaris* as Gram-negative bacteria and *S. mitis, S. salivarius, S. faecalis, S. aureus* as Gram-positive bacteria. Furthermore, ceftriaxone was used as a positive control. Minimum Inhibitory Concen-

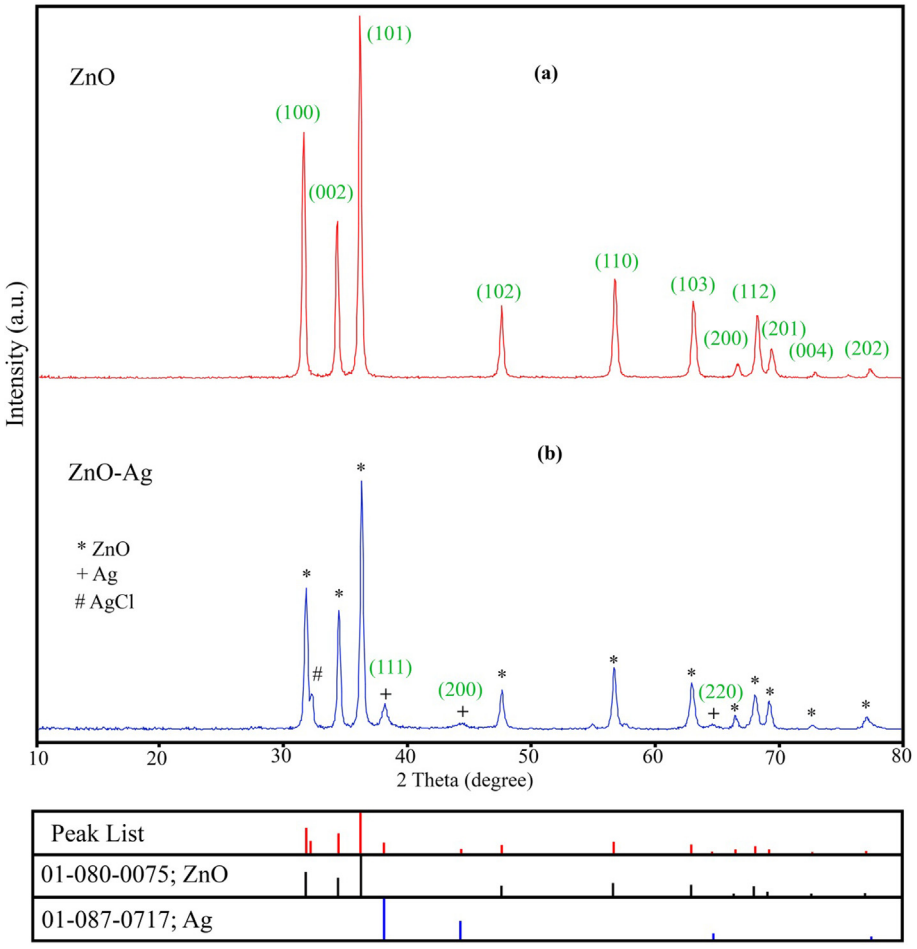

Fig. 2 XRD patterns of (a) pure ZnO NPs and (b) ZnO-Ag@CME NPs.

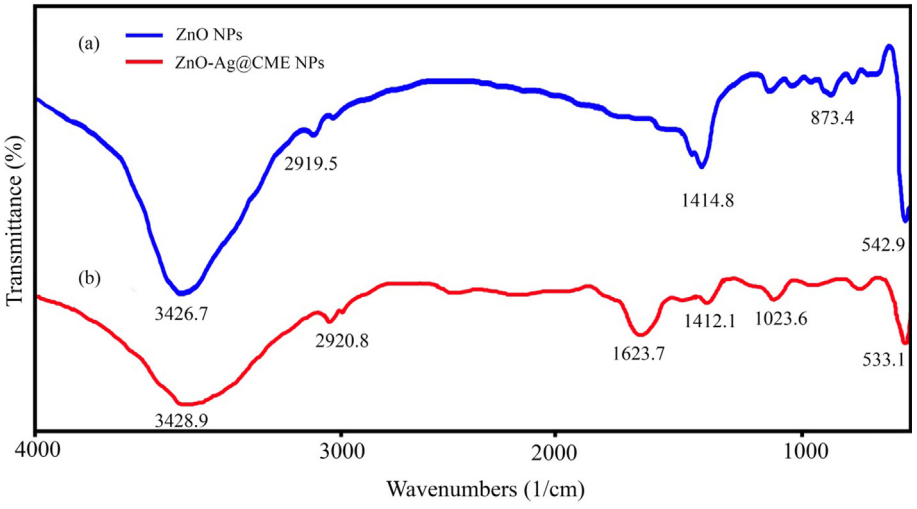

Fig. 3 FT-IR spectra of (a) pure ZnO NPs compared with (b) ZnO-Ag@CME NPs.

tration (MIC) of synthesized ZnO-Ag@CME NPs was determined by micro-dilution method and according to Shirzadi *et al.* (Shirzadi-Ahodashti et al., 2020) with slight modifications. MIC experiment was done in the 96-micro plate in triple set. Obtained nanoparticles at different concentrations (0.097 up to 200 µg/mL) were prepared in wells with 100 µl volume in the presence of Tryptic Soy Broth (TBS) medium. From each dilution, 100 µl was added to sterile microplate wells containing 100 µl of bacterial suspension and culture medium (equivalent to 0.5 McFarland concentrations diluted 1/150). Finally, the microplate was placed in an incubator at 37 ℃ and MIC was obtained after 24 h. Measuring the minimum

bactericidal concentration (MBC), 25 µl was taken from the wells without turbidity in completely sterile conditions and inoculated for 24 h at 37 ℃.

2.6. Photocatalytic activity

Photocatalysis experiments were carried out by modification of a previous study (Ebrahimzadeh et al., 2020). The photocatalytic activity of synthesized ZnO-Ag@CME NPs was investigated by monitoring the photodegradation of methyl orange (MO) as an anionic pollutant and basic violet 10 (BV10) as a cationic pollutant in an aqueous solution. The catalytic experiment was performed by using a contaminants aqueous solution (1.4 mg), including 40 mg of ZnO-Ag@CME NPs as nanocatalyst in the glass reactor. This mixture was aerated for reaching adsorption–desorption equilibrium for 30 min. Then, each colloidal mixture was irradiated by Osram lamp (150 W) and UV light (400 W). The Osram lamp was applied as an irradiance origin including a wavelength between visible lamp (400–700 nm) and UV lamp (250–400 nm) for the photocatalytic procedure. Maximum absorbance of contaminants was gathered using UV/Vis analysis (554 for BV10 and 464 for MO). The MO and BV10 pollutants degradation efficiency has been computed as follow:

$$\text{D.P.}(t) = \frac{A_0 - A_t}{A_0} \times 100 \quad (5)$$

where A_0 and A_t are absorbance amounts of dyes solutions before and after degradation, respectively.

2.7. Characterization

Functional groups present in the biosynthesized samples were determined using Fourier transform infrared spectrometer

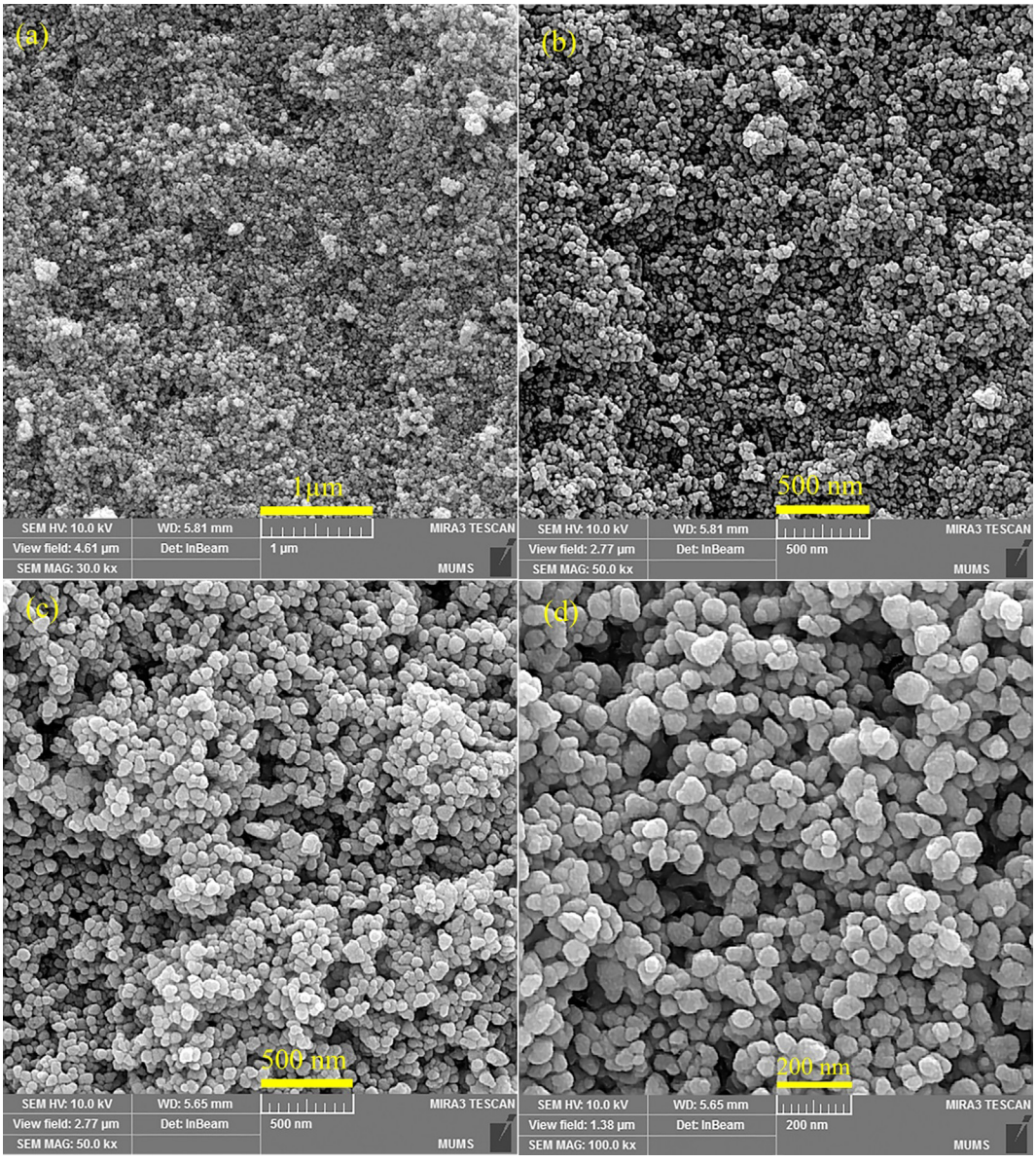

Fig. 4 The FESEM micrographs of (a and b) pure ZnO NPs and (c and d) ZnO-Ag@CME NPs.

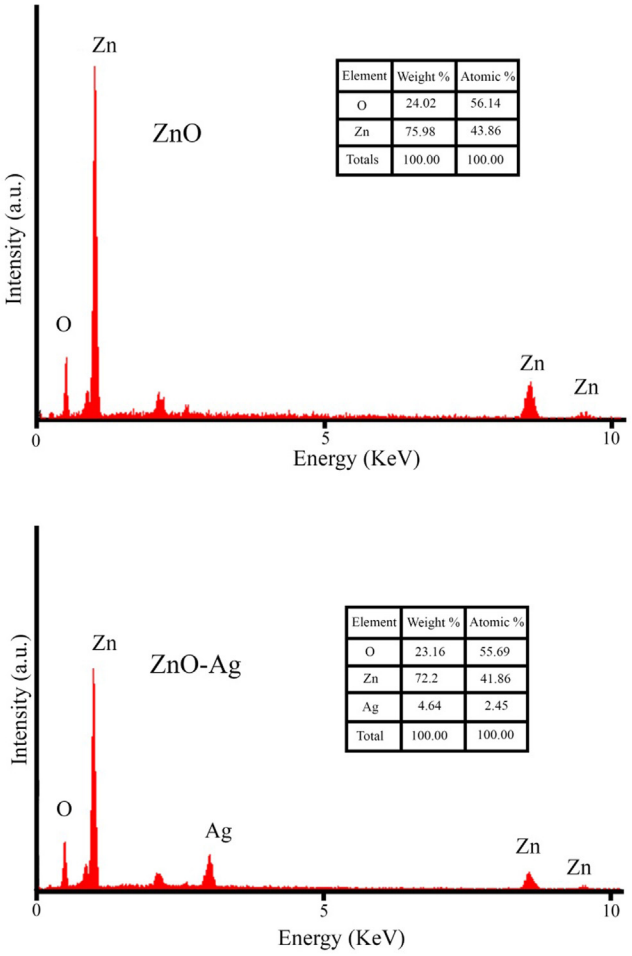

Fig. 5 EDS data of green synthesized pure ZnO NPs and ZnO-Ag@CME NPs.

(FT-IR; PerkinElmer Spectrum Two™ IR spectrometer; Model L160000U). The morphological structure and grain size of the ZnO and ZnO-Ag were analyzed by field emission scanning electron microscopy (FESEM; TESCAN BRNO-Mira3 LMU), and transmission electron microscopy (TEM; Zeiss-EM10C-100 KV). The crystallinity and structural characteristics of products were recorded using X-ray diffraction patterns (XRD; $2\theta = 10°–80°$, Philips PW 1800 using Cu Kα radiation). The EDS analysis was studied by XL30, Philips microscope. The hydrodynamic particle size analysis was performed by dynamic light-scattering (DLS) using Nano-Brook 90Plus-Brookhaven (model 18051; USA). Diffuse reflectance spectroscopy (DRS; Shimadzu, UV- 2550) was used to obtain reflectance spectra of the products for wavelengths between 300 and 800 nm.

3. Results and discussion

3.1. XRD analysis

The purity, crystallinity and phase of the synthesized products were determined by powder X-ray diffraction (XRD) analysis. XRD patterns of ZnO and ZnO-Ag nanoparticles are shown in Fig. 2. The XRD pattern of ZnO nanoparticles revealed in

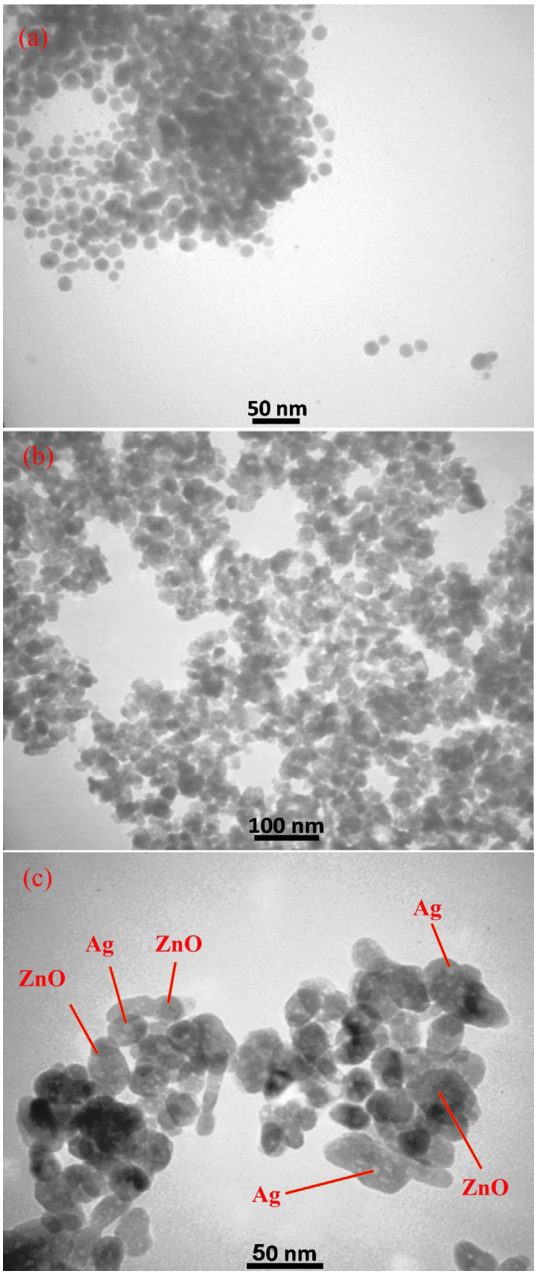

Fig. 6 Transmission electron microscopy (TEM) images of (a) pure ZnO NPs and (b and c) synthesized ZnO-Ag NPs in presence of *C. monogyna* extract at different magnification scales.

Fig. 2a with crystal structure as the hexagonal phase of the zinc oxide nanoparticles with unit cell parameters a = 3.25, b = 3.25, c = 5.2, p63mc space group (JCPDS No. 01–080-0075). Eleven major reflection peaks are showed at $2\theta = 31.88°$, 34.55°, 36.38°, 47.67°, 56.7°, 62.97°, 66.49°, 68.05°, 69.18°, 72.67°, and 75.35° that can be attributed to (100), (002), (101), (102), (110), (103), (200), (112), (201), (004), and (202) Miller indices (Wali, 2019). This pattern was matched very well to the XRD pattern of hexagonal type zinc oxide structure. Fig. 2b, shows the XRD pattern of ZnO-Ag@CME NPs. In addition to the ZnO peaks, the three additional peaks at 38.23° (111), 44.37° (200), and 64.56° (220) can be related to a cubic silver structure (JCPDS No. 01-

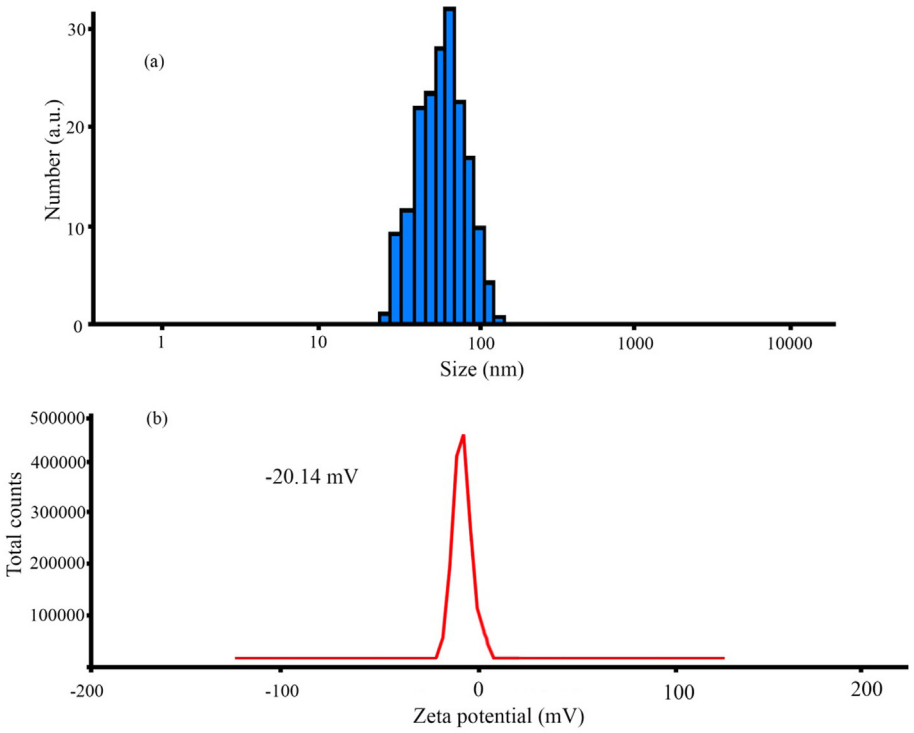

Fig. 7 DLS (a) and zeta potential (b) measurement of ZnO-Ag@CME NPs.

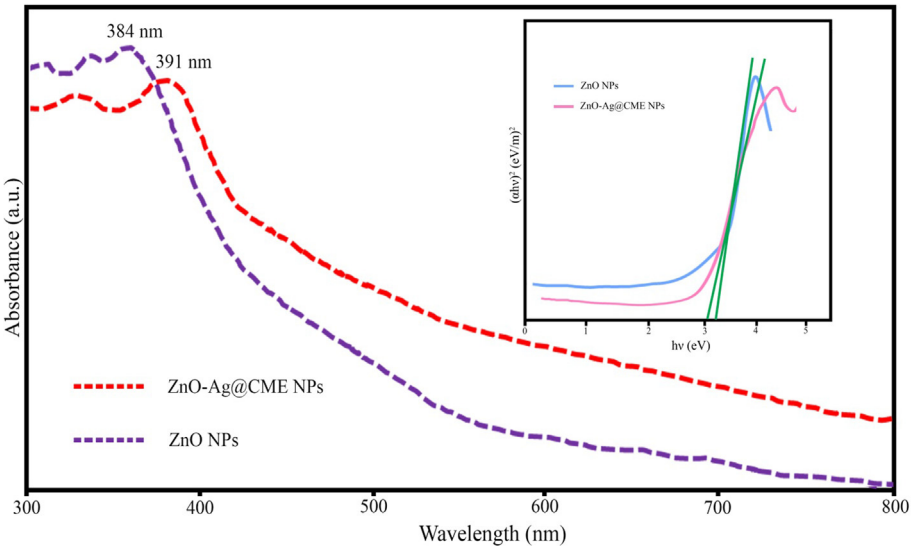

Fig. 8 UV/Vis analysis of pure ZnO NPs and ZnO-Ag NPs synthesized by *C. monogyna* extract.

087-0717). The diffraction peaks confirmed the formation of silver nanoparticles on the ZnO surface. The results were consistent with previous studies (Zhao et al., 2015; Kadam et al., 2018). The crystallite size of the product was measured using Debye-Scherrer equation: D (nm) = $0.9\lambda/\beta\text{Cos}\theta$ (6); where β is the FWHM (Full width at half maximum), λ is X-ray wavelength of Cu-Kα (1.5406 Å), and θ is the diffraction angle of the particles. The average size of pure ZnO and ZnO-Ag@CME NPs was determined to be 33.8 and 49.6 nm, respectively.

3.2. Fourier transform infrared spectra (FT-IR)

FT-IR spectrum is the best analysis to confirm the existence of various groups on the surface of products. FT-IR spectra of pure ZnO and ZnO-Ag@CME NPs are shown in Fig. 3. In FT-IR spectra (Fig. 3a) of ZnO NPs prepared by co-precipitate method, major bands appeared at 3426.7, 2919.5, 1414.8, 873.4, and 542.9 cm^{-1}. The characteristic absorption bands of zinc oxide at 3426.7, and 1414.8 cm^{-1} are related to O-H group of water molecules in ZnO NPs. The absorption

Table 2 MIC and MBC values (μg/mL) for ZnO-Ag@CME NPs tested against various microorganims.

Strain	ZnO-Ag NPs		Ceftriaxone	
	MIC (μg/mL)	MBC (μg/mL)	MIC (μg/mL)	MBC (μg/mL)
P. aeruginosa ATCC 27853	200	200	97.65	195.31
K. pneumoniae ATCC 9997	50	100	12.20	24.41
S. typhimurium ATCC 14028	12.5	50	390.62	781.25
P. vulgaris ATCC 6380	50	100	24.41	24.41
S. mitis ATCC 6249	12.5	25	48.82	1562.5
S. salivarius ATCC 1448	100	200	24.41	24.41
S. faecalis ATCC 15753	12.5	50	195.31	781.25
S. aureus ATCC 16538	200	400	390.62	1562.5

peak at 2919.5 cm^{-1} could be attributed to the stretching vibration of C-H (Azizi et al., 2016). The presence of metal-oxygen (Zn-O) band can be confirmed by the peak observed about 542.9 cm^{-1}. After forming of silver nanoparticles on the surface of zinc oxide nanoparticles, the intensity of the ZnO peak was decreased. The weak bands in the range of 800 to 1623.7 cm^{-1} (Fig. 3b) related to the *C. monogyna* extract components on the surface of the ZnO-Ag NPs (Noohpisheh et al., 2020).

3.3. FESEM, EDS, and TEM analysis

The size and shape analysis of the prepared pure ZnO and ZnO-Ag were performed using field emission electron microscopy (FESEM), which is illustrated in Fig. 4. Fig. 4a and b exhibits the FESEM images of pure ZnO nanoparticles synthesized by co-precipitate method at various magnifications. Spherical morphology, small nanoparticles (in size range of 35–50 nm) with regular and homogenous structures was the characteristics of ZnO nanoparticles. Morphology and particle size of ZnO-Ag prepared by *C. monogyna* extract are shown in Fig. 4c and d. No remarkable changes in the shape were noticed when silver was modified on the surface of zinc oxide nanoparticles. The FESEM results showed the spherical-like morphology, good disperse, regular and small size with an average size of about 60 ± 5.5 nm. The elemental composition analysis of the synthesized ZnO and ZnO-Ag nanoparticles was further confirmed by the EDS technique (Fig. 5). The lines of Zn, O, and Ag are observed (Attia et al., 2020). The EDS analysis also confirmed that silver nanoparticles are completely modified on the zinc oxide surface. For further investigation, transmission electron microscopy analysis was applied to study the morphology and size of the products (ZnO and ZnO-Ag nanoparticles) (Fig. 6). The TEM images exhibited that the pure ZnO (Fig. 6a) and ZnO-Ag@CME NPs (Fig. 6b and c) were spherical, uniform and the sizes of these samples were 35–50 and 55–70 nm, respectively.

3.4. DLS analysis

The zeta potential and dynamic light scattering (DLS) distribution techniques were carried out to study stabilization and the size distribution of the biosynthesized nanoparticles (Fig. 7). The DLS analysis showed the hydrodynamic size of ZnO-Ag@CME NPs as 55–110 nm (Fig. 7a). The increase is due to the presence of *C. monogyna* extract around the ZnO-Ag NPs. The nanomaterials stability is directly proportional to the magnitude of the charge (Kolahalam et al., 2021). The colloidal solution of ZnO-Ag@CME NPs possessed high negative zeta potentials of about −20.14 mV, which confirmed the highly stable synthesized nanoparticles solution (Fig. 7b). The negative zeta potential of ZnO-Ag nanoparticles were reported in previous studies (Rajendran and Mani, 2020; Chitradevi et al., 2019). Previous study has shown that surfaces charge and shape of nanomaterials have considerable roles on efficiency of products. Therefore, homogeneous structure, regular shape and surface charge in the range of about positive charge (+30 mV) and negative charge (−30 mV) can be effective.

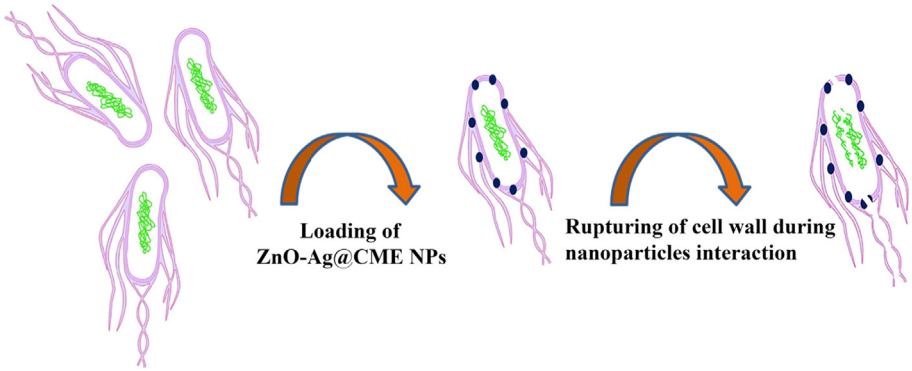

Scheme 2 **Representation** of possible antibacterial mechanism of silver nanoparticles.

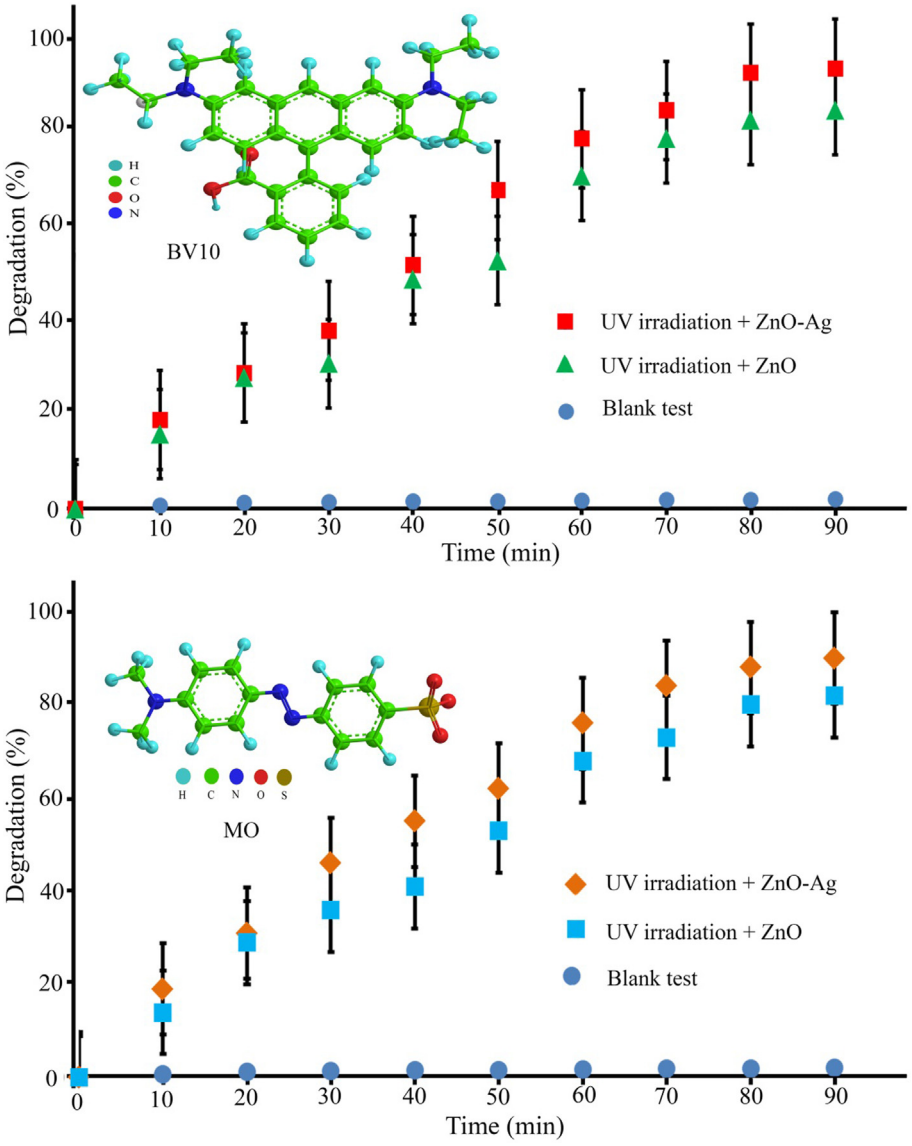

Fig. 9 Photocatalytic degradation of MO and BV10 hazardous pollutants under UV irradiation.

Apparently, this stability is because of the electrostatic repulsions among the individual particles.

3.5. Study of UV–Vis diffuse reflectance spectra

The diffuse reflectance spectra (UV–Vis) were determined to examine the light absorption properties of the biosynthesized pure ZnO NPs, and ZnO-Ag@CME NPs are revealed in Fig. 8. The synthesized pure ZnO NPs have an absorption edge around 384 nm, corresponding to a band-gap of 3.21 eV. Furthermore, the UV–Vis spectrum of ZnO-Ag@CME NPs showed a maximum absorption peak at 391 nm (Varadavenkatesan et al., 2019), which corresponds to a band-gap of 3.06 eV. According to the results, the presence of silver nanoparticles on the surface of ZnO NPs improves the band-gap absorption in comparison to the pure ZnO NPs. As shown in Fig. 8, the intensity of the absorption of pure ZnO NPs, decreased in the presence of silver nanoparticles. This can be explained via a reduction in the absorption of zinc oxide nanoparticles in the presence of silver nanoparticles.

3.6. Antibacterial activity

The ZnO-Ag@CME NPs were tested for their antibacterial activity against eight common microorganisms. Mueller Hinton broth process was applied to determine the antibacterial efficiency of synthesized nanoparticles. MIC and MBC values of the ZnO-Ag@CME NPs, and ceftriaxone as an antibiotic are summarized in Table 2. As revealed in Table 2, the MIC (minimum inhibitory concentration) of ZnO-Ag@CME NPs was found to be 200 μg/mL for *P. aeruginosa,* 50 μg/mL for *K. pneumoniae,* 12.5 μg/mL for *S. typhimurium,* 50 μg/mL for *P. vulgaris,* 12.5 for μg/mL *S. mitis,* 100 μg/mL for *S. salivarius,* 12.5 μg/mL for *S. faecalis,* and 200 μg/mL for *S. aureus*. In addition, the MBC values were recorded as follows: 200, 100, 50, 100, 25, 200, 50, and 400 μg/mL, respectively. In addition, the broad-spectrum antibiotic ceftriaxone had the great-

est effect on *K. pneumoniae*, *P. vulgaris* and *S. salivarius* with MIC value of 12.2, 24.41, 24.41 μg/mL, respectively and the least effect on *S. typhimurium* and *S. aureus* with MIC value of 390.62 μg/mL. These results illustrated that the ZnO-Ag synthesized from *C. monogyna* extract had excellent antibacterial activity against most bacteria. The biosynthesized ZnO-Ag using *C. monogyna* extract showed the highest antibacterial activity against *K. pneumoniae, S. typhimurium, P. vulgaris, S. mitis,* and *S. faecalis* and then against *S. aureus, S. salivarius,* and *P. aeruginosa* were found to be much less sensitive to synthesized ZnO-Ag@CME NPs. Up to now, the accurate anti-bacterial mechanism of metallic nanoparticles has not been confirmed yet. Many antibacterial mechanisms have been proposed such as the interaction of nanoparticles with bacteria to damaging the bacterial cell, and the formation of reactive oxygen species (ROS) (Stoimenov et al., 2002; Xia et al., 2008; Nel et al., 2006). However the most acceptable mechanism may involve as follow: (i) attachment of nanoparticles to the surface of the cell membrane (ii) penetration into bacteria (iii) and leading to death of cell (Scheme 2) (Thi Lan Huong and Nguyen, 2021).

3.7. Photocatalytic performance

The photocatalytic degradation of methyl orange (MO) and basic violet 10 (BV10) under irradiation with sunlight and UV irradiations were used to prove the photocatalytic efficiency of the synthesized pure ZnO and ZnO-Ag@CME NPs. Fig. 9 shows the photocatalytic degradation of hazardous pollutants in presence of ZnO and ZnO-Ag@CME NPs under UV irradiation. Very low degradation has occurred without the usage of the nanocatalyst under UV and sunlight irradiations. The MO degradation at 90 min of reaction applying nano-scale ZnO-Ag and pure ZnO was 89.8% and 80.1% under UV irradiation. Furthermore, the degradation efficiency of the BV10 contaminant was about 94.2% and 82.2% for ZnO-Ag@CME NPs and ZnO, respectively under UV irradiation after 90 min. The photocatalytic experiment was per-

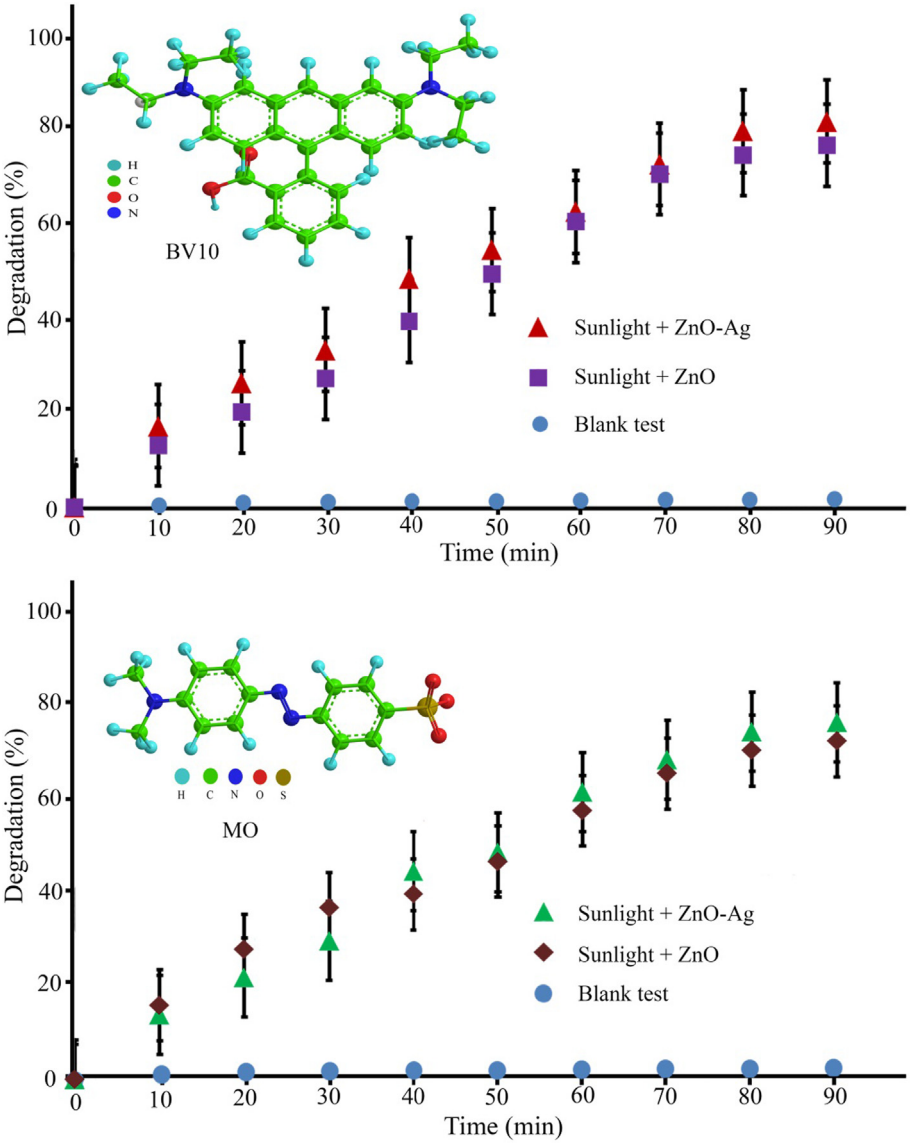

Fig. 10 Photocatalytic degradation of MO and BV10 organic contaminants under sunlight irradiation.

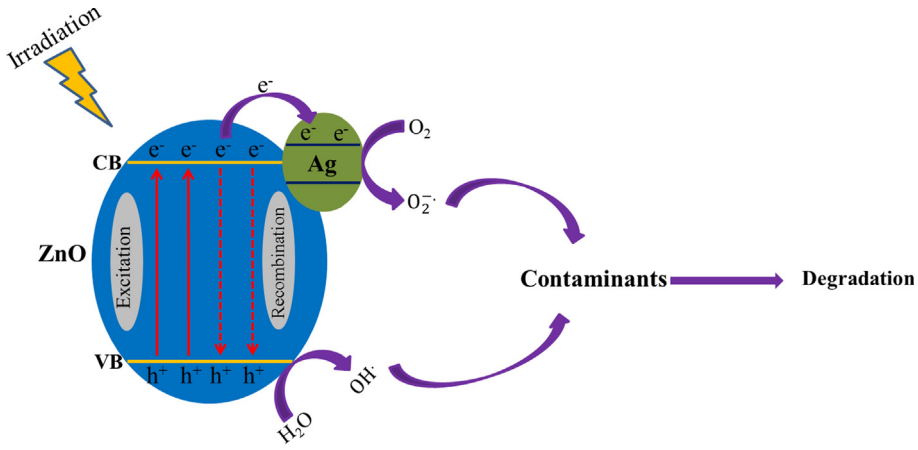

Scheme 3 **Probable** degradation mechanism of pollutants by ZnO-Ag@CME NPs under UV and sunlight irradiations.

formed under sunlight irradiation and the results are shown in Fig. 10. This value was significantly higher than the reported values. The photocatalytic degradation shows that the photodegradation of MO and BV10 pollutants were about (75.3% and 84.7%) and (67.4% and 76.5%) for ZnO-Ag@CME NPs and pure ZnO after 90 min irradiation of sunlight, respectively. To sum up, it can be concluded that the photocatalytic efficiency of ZnO-Ag@CME NPs was more than pure ZnO NPs. Appropriate absorption of visible light and low quantity of the energy gap were the reasons for this difference (Singh et al., 2014; Zhong et al., 2012). The photoexcited holes and electrons are formed in the valence band (VB) and the conduction band (CB) of silver nanoparticles. This phenomenon occurs after irradiated to the ZnO-Ag as nanocatalysts. After that, electron transfer from the conduction band of ZnO-Ag nanoparticles to the conduction band of silver nanoparticles. This phenomenon leads to a decrease in recombination and an increase in photocatalytic performance (Scheme 3). The proposed mechanism of photocatalytic activity could be explained as follow:

$$\text{ZnO-Ag} + h\nu \rightarrow \text{ZnO-Ag} + \quad + h^+ \tag{7}$$

$$h^+ + H_2O \rightarrow OH \tag{8}$$

$$e^- + O_2 \rightarrow O^-_2 \tag{9}$$

$$OH + O^-_2 + \text{pollutants} \rightarrow \text{degradation products} \tag{10}$$

4. Conclusion

In doing so, we provided a green, simple and cost-effective process for the synthesis of ZnO-Ag nanoparticles using *C. monogyna* extract as capping, stabilizing, and reducing agents. Characterizations were carried out using FT-IR, FESEM, TEM, EDS, and XRD techniques. The crystalline ZnO and ZnO-Ag@CME NPs were obtained in spherical morphology with mean sizes of 35–50 and 55–70 nm, respectively. The ZnO-Ag@CME NPs were used as nanocatalyst and found to be efficient in degradation of BV10 and MO pollutions in the presence of UV and sunlight irradiations. Results showed that the highest efficiency of BV10 (94.2% for UV and 84.7% for sunlight) and MO 89.8% for UV and 75.3% for sunlight) degradation (77%) occurred after 90 min. Furthermore, ZnO-Ag@CME NPs exhibited strong antibacterial activity against both Gram-positive and Gram-negative bacterial strains. Therefore, it can be concluded that synthesis of ZnO-Ag using *C. monogyna* extract could be very effective for utilization in environmental and biomedical fields.

Declaration of Competing Interest

The authors declare that they have no known competing financial interests or personal relationships that could have appeared to influence the work reported in this paper.

Acknowledgment

Funding this project was funded by research center for environmental pollutants, Qom University of Medical Sciences (Grant number: 991267).

References

Alabdallah, N.M., Hasan, M.M., 2021. Plant-based green synthesis of silver nanoparticles and its effective role in abiotic stress tolerance in crop plants. Saudi J. Biol. Sci.

Al-Asfar, A., Zaheer, Z., Aazam, E.S., 2018. Eco-friendly green synthesis of Ag@Fe bimetallic nanoparticles: antioxidant, antimicrobial and photocatalytic degradation of bromothymol blue. J. Photochem. Photobiol., B 185, 143–152.

Alomar, T.S., AlMasoud, N., Awad, M.A., El-Tohamy, M.F., Soliman, D.A., 2020. An eco-friendly plant-mediated synthesis of silver nanoparticles: characterization, pharmaceutical and biomedical applications. Mater. Chem. Phys. 249, 123007.

Ardestani, M.S., Bitarafan-Rajabi, A., Mohammadzadeh, P., Mortazavi-Derazkola, S., Sabzevari, O., Azar, A.D., Kazemi, S., Hosseini, S.R., Ghoreishi, S.M., 2020. Synthesis and characterization of novel 99mTc-DGC nano-complexes for improvement of heart diagnostic. Bioorg. Chem. 96.

Arumugam, M., Manikandan, D.B., Dhandapani, E., Sridhar, A., Balakrishnan, K., Markandan, M., Ramasamy, T., 2021. Green synthesis of zinc oxide nanoparticles (ZnO NPs) using Syzygium cumini: potential multifaceted applications on antioxidants, cytotoxic and as nanonutrient for the growth of Sesamum indicum. Environ. Technol. Innovation 23, 101653.

Attia, Y.A., Mohamed, Y.M.A., Awad, M.M., Alexeree, S., 2020. Ag doped ZnO nanorods catalyzed photo-triggered synthesis of some

novel (1H-tetrazol-5-yl)-coumarin hybrids. J. Organomet. Chem. 919, 121320.
Azizi, S., Mohamad, R., Rahim, R.A., Moghaddam, A.B., Moniri, M., Ariff, A., Saad, W.Z., Namvab, F., 2016. ZnO-Ag core shell nanocomposite formed by green method using essential oil of wild ginger and their bactericidal and cytotoxic effects. Appl. Surf. Sci. 384, 517–524.
Bhanja, S.K., Samanta, S.K., Mondal, B., Jana, S., Ray, J., Pandey, A., Tripathy, T., 2020. Green synthesis of Ag@Au bimetallic composite nanoparticles using a polysaccharide extracted from Ramaria botrytis mushroom and performance in catalytic reduction of 4-nitrophenol and antioxidant, antibacterial activity. Environ. Nanotechnol. Monit. Manage. 14, 100341.
Cahyana, A.H., Liandi, A.R., Yulizar, Y., Romdoni, Y., Wendari, T. P., 2021. Green synthesis of $CuFe_2O_4$ nanoparticles mediated by Morus alba L. leaf extract: Crystal structure, grain morphology, particle size, magnetic and catalytic properties in Mannich reaction. Ceram. Int. 47, 21373–21380.
Chennimalai, M., Vijayalakshmi, V., Senthil, T.S., Sivakumar, N., 2021. One-step green synthesis of ZnO nanoparticles using Opuntia humifusa fruit extract and their antibacterial activities. Mater. Today:. Proc.
Chitradevi, T., Jestin Lenus, A., Victor Jaya, N., 2019. Structure, morphology and luminescence properties of sol-gel method synthesized pure and Ag-doped ZnO nanoparticles. Mater. Res. Express 7, 015011.
Ebrahimzadeh, M.A., Mortazavi-Derazkola, S., Zazouli, M.A., 2019. Eco-friendly green synthesis and characterization of novel Fe_3O_4/SiO_2/Cu_2O–Ag nanocomposites using Crataegus pentagyna fruit extract for photocatalytic degradation of organic contaminants. J. Mater. Sci.: Mater. Electron. 30, 10994–11004.
Ebrahimzadeh, M.A., Mortazavi-Derazkola, S., Zazouli, M.A., 2020. Eco-friendly green synthesis of novel magnetic Fe_3O_4/SiO_2/ZnO-Pr_6O_{11} nanocomposites for photocatalytic degradation of organic pollutant. J. Rare Earths 38, 13–20.
Ebrahimzadeh, M.A., Naghizadeh, A., Mohammadi-Aghdam, S., Khojasteh, H., Ghoreishi, S.M., Mortazavi-Derazkola, S., 2020. Enhanced catalytic and antibacterial efficiency of biosynthesized Convolvulus fruticosus extract capped gold nanoparticles (CFE@AuNPs). J. Photochem. Photobiol., B 209.
Ebrahimzadeh, M.A., Hashemi, Z., Mohammadyan, M., Fakhar, M., Mortazavi-Derazkola, S., 2021. In vitro cytotoxicity against human cancer cell lines (MCF-7 and AGS), antileishmanial and antibacterial activities of green synthesized silver nanoparticles using Scrophularia striata extract. Surf. Interfaces 23, 100963.
Elijah, O., Nwabanne, T., 2014. Adsorption studies on the removal of Eriochrome black-T from aqueous solution using Nteje clay.
Eslami, H., Ehrampoush, M.H., Esmaeili, A., Salmani, M.H., Ebrahimi, A.A., Ghaneian, M.T., Falahzadeh, H., Fard, R.F., 2019. Enhanced coagulation process by Fe-Mn bimetal nano-oxides in combination with inorganic polymer coagulants for improving As(V) removal from contaminated water. J. Cleaner Prod. 208, 384–392.
Ghanbari, D., Sharifi, S., Naraghi, A., Nabiyouni, G., 2016. Photo-degradation of azo-dyes by applicable magnetic zeolite Y-Silver–$CoFe_2O_4$ nanocomposites. J. Mater. Sci.: Mater. Electron. 27, 5315–5323.
Ghoreishi, S.M., Khalaj, A., Bitarafan-Rajabi, A., Azar, A.D., Ardestani, M.S., Assadi, A., 2017. Novel 99mTc-radiolabeled anionic linear globular PEG-based dendrimer-chlorambucil: non-invasive method for in-vivo biodistribution. Drug research 67, 149–155.
Gonca, S., Isik, Z., Özdemir, S., Arslan, H., Dizge, N., 2021. The surface modification of ultrafiltration membrane with silver nanoparticles using Verbascum thapsus leaf extract using green synthesis phenomena. Surf. Interfaces, 101291.
Goutam, S.P., Saxena, G., Singh, V., Yadav, A.K., Bharagava, R.N., Thapa, K.B., 2018. Green synthesis of TiO2 nanoparticles using leaf extract of Jatropha curcas L. for photocatalytic degradation of tannery wastewater. Chem. Eng. J. 336, 386–396.
Heinemann, M.G., Rosa, C.H., Rosa, G.R., Dias, D., 2021. Biogenic synthesis of gold and silver nanoparticles used in environmental applications: a review. Trends Environ. Anal. Chem. 30, e00129.
Joulaei, M., Hedayati, K., Ghanbari, D., 2019. Investigation of magnetic, mechanical and flame retardant properties of polymeric nanocomposites: green synthesis of $MgFe_2O_4$ by lime and orange extracts. Compos. B Eng. 176, 107345.
Kadam, A.N., Bhopate, D.P., Kondalkar, V.V., Majhi, S.M., Bathula, C.D., Tran, A.-V., Lee, S.-W., 2018. Facile synthesis of Ag-ZnO core–shell nanostructures with enhanced photocatalytic activity. J. Ind. Eng. Chem. 61, 78–86.
Kaplan, Ö., Gökşen Tosun, N., Özgür, A., Erden Tayhan, S., Bilgin, S., Türkekul, İ., Gökce, İ., 2021. Microwave-assisted green synthesis of silver nanoparticles using crude extracts of Boletus edulis and Coriolus versicolor: characterization, anticancer, antimicrobial and wound healing activities. J. Drug Delivery Sci. Technol. 64, 102641.
Khatami, M., Varma, R.S., Zafarnia, N., Yaghoobi, H., Sarani, M., Kumar, V.G., 2018. Applications of green synthesized Ag, ZnO and Ag/ZnO nanoparticles for making clinical antimicrobial wound-healing bandages. Sustainable Chem. Pharmacy 10, 9–15.
Kiani, A., Nabiyouni, G., Masoumi, S., Ghanbari, D., 2019. A novel magnetic $MgFe_2O4$–$MgTiO_3$ perovskite nanocomposite: rapid photo-degradation of toxic dyes under visible irradiation. Compos. B Eng. 175, 107080.
Kolahalam, L.A., Prasad, K.R.S., Murali Krishna, P., Supraja, N., 2021. Saussurea lappa plant rhizome extract-based zinc oxide nanoparticles: synthesis, characterization and its antibacterial, antifungal activities and cytotoxic studies against Chinese Hamster Ovary (CHO) cell lines. Heliyon 7, e07265.
Kumar, V.B., Annamanedi, M., Prashad, M.D., Arunasree, K.M., Mastai, Y., Gedanken, A., Paik, P., 2013. Synthesis of mesoporous SiO_2–ZnO nanocapsules: encapsulation of small biomolecules for drugs and "SiOZO-plex" for gene delivery. J. Nanopart. Res. 15, 1904.
Lam, S.-M., Sin, J.-C., Zeng, H., Lin, H., Li, H., Chai, Y.-Y., Choong, M.-K., Mohamed, A.R., 2021. Green synthesis of Fe-ZnO nanoparticles with improved sunlight photocatalytic performance for polyethylene film deterioration and bacterial inactivation. Mater. Sci. Semicond. Process. 123, 105574.
Malik, M.A., Alshehri, A.A., Patel, R., 2021. Facile one-pot green synthesis of Ag–Fe bimetallic nanoparticles and their catalytic capability for 4-nitrophenol reduction. J. Mater. Res. Technol. 12, 455–470.
Manjari, G., Saran, S., Radhakrishanan, S., Rameshkumar, P., Pandikumar, A., Devipriya, S.P., 2020. Facile green synthesis of Ag–Cu decorated ZnO nanocomposite for effective removal of toxic organic compounds and an efficient detection of nitrite ions. J. Environ. Manage. 262, 110282.
Mehta, R.V., 2017. Synthesis of magnetic nanoparticles and their dispersions with special reference to applications in biomedicine and biotechnology. Mater. Sci. Eng., C 79, 901–916.
Mohammadi-Aghdam, S., Valinezhad-Saghezi, B., Mortazavi, Y., Qhoreishi, S.M., 2019. Modified Fe_3O_4/HAp magnetically nanoparticles as the carrier for ibuprofen: adsorption and release study. Drug Res. 69, 93–99.
Moraes, L.C., Figueiredo, R.C., Ribeiro-Andrade, R., Pontes-Silva, A. V., Arantes, M.L., Giani, A., Figueredo, C.C., 2021. High diversity of microalgae as a tool for the synthesis of different silver nanoparticles: a species-specific green synthesis. Colloid Interface Sci. Commun. 42, 100420.
Mortazavi-Derazkola, S., Naimi-Jamal, M.R., Ghoreishi, S.M., 2016. Synthesis, characterization, and atenolol delivery application of functionalized mesoporous hydroxyapatite nanoparticles prepared by microwave-assisted co-precipitation method. Curr. Drug Deliv. 13, 1123–1129.

Naghizadeh, A., Mizwari, Z.M., Ghoreishi, S.M., Lashgari, S., Mortazavi-Derazkola, S., Rezaie, B., 2021. Biogenic and eco-benign synthesis of silver nanoparticles using jujube core extract and its performance in catalytic and pharmaceutical applications: removal of industrial contaminants and in-vitro antibacterial and anticancer activities. Environ. Technol. Innovation 23, 101560.

Najjar, M., Hosseini, H.A., Masoudi, A., Sabouri, Z., Mostafapour, A., Khatami, M., Darroudi, M., 2021. Green chemical approach for the synthesis of SnO2 nanoparticles and its application in photocatalytic degradation of Eriochrome Black T dye. Optik 242, 167152.

Nel, A., Xia, T., Mädler, L., Li, N., 2006. Toxic potential of materials at the nanolevel. Science (New York, N.Y.) 311, 622–627.

Nga, N.K., Thuy Chau, N.T., Viet, P.H., 2018. Facile synthesis of hydroxyapatite nanoparticles mimicking biological apatite from eggshells for bone-tissue engineering. Colloids Surf., B 172, 769–778.

Noohpisheh, Z., Amiri, H., Farhadi, S., Mohammadi-gholami, A., 2020. Green synthesis of Ag-ZnO nanocomposites using Trigonella foenum-graecum leaf extract and their antibacterial, antifungal, antioxidant and photocatalytic properties. Spectrochim. Acta Part A Mol. Biomol. Spectrosc. 240, 118595.

Olajire, A.A., Mohammed, A.A., 2019. Green synthesis of palladium nanoparticles using Ananas comosus leaf extract for solid-phase photocatalytic degradation of low density polyethylene film. J. Environ. Chem. Eng. 7, 103270.

Pandiyan, N., Murugesan, B., Arumugam, M., Sonamuthu, J., Samayanan, S., Mahalingam, S., 2019. Ionic liquid - A greener templating agent with Justicia adhatoda plant extract assisted green synthesis of morphologically improved Ag-Au/ZnO nanostructure and it's antibacterial and anticancer activities. J. Photochem. Photobiol., B 198, 111559.

Pandiyan, N., Murugesan, B., Arumugam, M., Chinnaalagu, D., Samayanan, S., Mahalingam, S., 2021. Ionic liquid mediated green synthesis of Ag-Au/Y_2O_3 nanoparticles using leaves extracts of Justicia adhatoda: structural characterization and its biological applications. Adv. Powder Technol. 32, 2213–2225.

Perveen, R., Shujaat, S., Qureshi, Z., Nawaz, S., Khan, M.I., Iqbal, M., 2020. Green versus sol-gel synthesis of ZnO nanoparticles and antimicrobial activity evaluation against panel of pathogens. J. Mater. Res. Technol. 9, 7817–7827.

Rajendran, R., Mani, A., 2020. Photocatalytic, antibacterial and anticancer activity of silver-doped zinc oxide nanoparticles. J. Saudi Chem. Soc. 24, 1010–1024.

Rao, T.N., Riyazuddin, P., Babji, N., Ahmad, R.A., Khan, I., Hassan, S.A., Shahzad, F.M., 2019. Husain, Green synthesis and structural classification of Acacia nilotica mediated-silver doped titanium oxide (Ag/TiO_2) spherical nanoparticles: assessment of its antimicrobial and anticancer activity. Saudi J. Biol. Sci. 26, 1385–1391.

Şahin, Ö., Saka, C., Kutluay, S., 2013. Cold plasma and microwave radiation applications on almond shell surface and its effects on the adsorption of Eriochrome Black T. J. Ind. Eng. Chem. 19, 1617–1623.

Salehi, H., Ebrahimi, A.A., Ehrampoush, M.H., Salmani, M.H., Fard, R.F., Jalili, M., Gholizadeh, A., 2020. Integration of photo-oxidation based on UV/Persulfate and adsorption processes for arsenic removal from aqueous solutions. Groundwater Sustainable Dev. 10, 100338.

Saravanadevi, K., Kavitha, M., Karpagavinayagam, P., Saminathan, K., Vedhi, C., 2020. Biosynthesis of ZnO and Ag doped ZnO nanoparticles from Vitis vinifera leaf for antibacterial, photocatalytic application. Mater. Today:. Proc.

Shaikshavali, P., Madhusudana Reddy, T., Venu Gopal, T., Venkataprasad, G., Kotakadi, V.S., Palakollu, V.N., Karpoormath, R., 2020. A simple sonochemical assisted synthesis of nanocomposite (ZnO/MWCNTs) for electrochemical sensing of Epinephrine in human serum and pharmaceutical formulation. Colloids Surf., A 584, 124038.

Shirzadi-Ahodashti, M., Ebrahimzadeh, M.A., Ghoreishi, S.M., Naghizadeh, A., Mortazavi-Derazkola, S., 2020. Facile and eco-benign synthesis of a novel $MnFe_2O_4$@SiO_2@Au magnetic nanocomposite with antibacterial properties and enhanced photocatalytic activity under UV and visible-light irradiations. Appl. Organomet. Chem. 34.

Shirzadi-Ahodashti, M., Mortazavi-Derazkola, S., Ebrahimzadeh, M. A., 2020. Biosynthesis of noble metal nanoparticles using crataegus monogyna leaf extract (CML@X-NPs, X = Ag, Au): antibacterial and cytotoxic activities against breast and gastric cancer cell lines. Surf. Interfaces 21, 100697.

Shirzadi-Ahodashti, M., Mizwari, Z.M., Hashemi, Z., Rajabalipour, S., Ghoreishi, S.M., Mortazavi-Derazkola, S., Ebrahimzadeh, M. A., 2021. Discovery of high antibacterial and catalytic activities of biosynthesized silver nanoparticles using C. fruticosus (CF-AgNPs) against multi-drug resistant clinical strains and hazardous pollutants. Environ. Technol. Innovation 23, 101607.

Singh, L.P., Luwang, M.N., Srivastava, S.K., 2014. Luminescence and photocatalytic studies of Sm3 + ion doped SnO2 nanoparticles. New J. Chem. 38, 115–121.

Sridar, R., Ramanane, U.U., Rajasimman, M., 2018. ZnO nanoparticles – synthesis, characterization and its application for phenol removal from synthetic and pharmaceutical industry wastewater. Environ. Nanotechnol. Monit. Manage. 10, 388–393.

Stoimenov, P.K., Klinger, R.L., Marchin, G.L., Klabunde, K.J., 2002. Metal oxide nanoparticles as bactericidal agents. Langmuir 18, 6679–6686.

Suba, S., Vijayakumar, S., Vidhya, E., Punitha, V.N., Nilavukkarasi, M., 2021. Microbial mediated synthesis of ZnO nanoparticles derived from Lactobacillus spp: Characterizations, antimicrobial and biocompatibility efficiencies. Sensors International 2, 100104.

Thi Lan Huong, V., Nguyen, N.T., 2021. Green synthesis, characterization and antibacterial activity of silver nanoparticles using Sapindus mukorossi fruit pericarp extract. Mater. Today: Proc. 42, 88–93.

Tiwari, V., Mishra, N., Gadani, K., Solanki, P.S., Shah, N.A., Tiwari, M., 2018. Mechanism of anti-bacterial activity of zinc oxide nanoparticle against Carbapenem-Resistant Acinetobacter baumannii. Front. Microbiol. 9, 1218.

Varadavenkatesan, T., Lyubchik, E., Pai, S., Pugazhendhi, A., Vinayagam, R., Selvaraj, R., 2019. Photocatalytic degradation of Rhodamine B by zinc oxide nanoparticles synthesized using the leaf extract of Cyanometra ramiflora. J. Photochem. Photobiol., B 199, 111621.

Vasantharaj, S., Sathiyavimal, S., Senthilkumar, P., Kalpana, V.N., Rajalakshmi, G., Alsehli, M., Elfasakhany, A., Pugazhendhi, A., 2021. Enhanced photocatalytic degradation of water pollutants using bio-green synthesis of zinc oxide nanoparticles (ZnO NPs). J. Environ. Chem. Eng. 9, 105772.

Wali, M., 2019. Optical, morphological and biological analysis of zinc oxide nanoparticles (ZnO NPs) using Papaver somniferum L, RSC advances, 9, 29541-29548-22019 v.29549 no.29551.

Wang, Z., Ye, X., Chen, L., Huang, P., Wang, Q., Ma, L., Hua, N., Liu, X., Xiao, X., Chen, S., 2021. Silver nanoparticles decorated grassy ZnO coating for photocatalytic activity enhancement. Mater. Sci. Semicond. Process. 121, 105354.

Xia, T., Kovochich, M., Liong, M., Mädler, L., Gilbert, B., Shi, H., Yeh, J.I., Zink, J.I., Nel, A.E., 2008. Comparison of the mechanism of toxicity of zinc oxide and cerium oxide nanoparticles based on dissolution and oxidative stress properties. ACS Nano 2, 2121–2134.

Yilmaz, M.T., İspirli, H., Taylan, O., Dertli, E., 2020. Synthesis and characterisation of alternan-stabilised silver nanoparticles and determination of their antibacterial and antifungal activities against foodborne pathogens and fungi. LWT 128, 109497.

Yin, I.X., Zhang, J., Zhao, I.S., Mei, M.L., Li, Q., Chu, C.H., 2020. The antibacterial mechanism of silver nanoparticles and its application in dentistry. Int. J. Nanomed. 15, 2555–2562.

Zare-Akbari, Z., Farhadnejad, H., Furughi-Nia, B., Abedin, S., Yadollahi, M., Khorsand-Ghayeni, M., 2016. PH-sensitive bionanocomposite hydrogel beads based on carboxymethyl cellulose/ZnO nanoparticle as drug carrier. Int. J. Biol. Macromol. 93, 1317–1327.

Zhao, Z.-Y., Wang, M.-H., Liu, T.-T., 2015. Tribulus terrestris leaf extract assisted green synthesis and gas sensing properties of Ag-coated ZnO nanoparticles. Mater. Lett. 158, 274–277.

Zhong, J.B., Li, J.Z., Feng, F.M., Lu, Y., Zeng, J., Hu, W., Tang, Z., 2012. Improved photocatalytic performance of SiO2–TiO2 prepared with the assistance of SDBS. J. Mol. Catal. A: Chem. 357, 101–105.

Zulkifli, F.H., Hussain, F.S.J., Zeyohannes, S.S., Rasad, M.S.B.A., Yusuff, M.M., 2017. A facile synthesis method of hydroxyethyl cellulose-silver nanoparticle scaffolds for skin tissue engineering applications. Mater. Sci. Eng., C 79, 151–160.